Magnetic structures in a dhcp samarium film

C. Dufour, K. Dumesnil, S. Soriano, and Ph. Mangin
Laboratoire de Physique des Matériaux (UMR CNRS 7556), University H. Poincaré - Nancy I, Boîte Postale 239, F-54506 Vandoeuvre cedex, France

P. J. Brown and A. Stunault
ILL, Boîte Postale 156X, F-38042 Grenoble cedex 9, France

N. Bernhoeft
CENG, DRFMC/SPSMS/MRS, F-38054 Grenoble cedex, France
(Received 17 May 2002; published 25 September 2002)

Thick samarium films with a four plane dhcp structure instead of the nine-layer stacking characteristic of the element in bulk form, have been prepared by molecular-beam epitaxy. The magnetic structure of this dhcp phase has been elucidated using both neutron-scattering and resonant x-ray magnetic scattering experiments. The magnetic moments align along the *c* direction. In a given basal plane, for the hexagonal (*h*) sites as well as for the cubic (*c*) sites, the magnetic ordering is the same as in bulk samarium. However, the three-dimensional magnetic ordering is modified compared to the bulk one, since both types of planes (*h* and *c*) couple antiferromagnetically along the *c* axis. Moreover, both sets of sites order nearly simultaneously at about 25 K. Compared to bulk, the magnetic ordering temperature is thus lower for the hexagonal sites and higher for the cubic ones.

DOI: 10.1103/PhysRevB.66.094428 PACS number(s): 75.25.+z, 75.70.−i

INTRODUCTION

Among other rare earths, samarium is an atypical element with respect to its crystal structure and its electronic and magnetic properties. In the lanthanide series, it lies between the dhcp light rare earths and the hcp heavy ones. At atmospheric pressure and for temperatures lower than 1197 K, it exhibits an exotic crystal structure with rhombohedral symmetry:[1] the hexagonal chemical cell ($a=3.6291$ Å and $c=26.203$ Å) can be described as a stack of nine close-packed planes. This structure (referred to as the ''Sm structure'') shows two sublattices of sites, with hexagonal (*h*) or cubic (*c*) symmetry that stack in a ($hhchhc\ldots$) sequence along the crystal *c* direction. Two modulated magnetic phases, associated to the magnetic moments localized on the hexagonal and cubic sites, order successively and independently below 106 K and 13.8 K, respectively.[2–5] The magnetic arrangement obeys the following rules.

(i) The moments on both types of sites align along the *c* direction.

(ii) The magnetic order is ferromagnetic within the hexagonal planes.

(iii) The hexagonal planes are antiferromagnetically coupled in a ($++0--0\ldots$) sequence along the *c* axis. The propagation vector is $\boldsymbol{\tau}_h=(0\ 0\ 1.5)$.

(iv) In each cubic plane, the moments form ferromagnetic rows parallel to one of the *a* directions with a ($++--+ +\ldots$) sequence along the other two.

(v) Although successive cubic planes are separated by two hexagonal planes (≈ 9 Å), they also couple in a three-dimensional order that is characterized by a propagation vector $\boldsymbol{\tau}_c=(0.25\ 0\ 0.75)$.

Samarium is known to undergo pressure- and/or temperature-induced crystallographic phase transformations to dhcp, hcp, bcc, and fcc structures. A complete temperature-pressure diagram has been proposed by Coles.[6] However the magnetic behavior of samarium in allotropes different from the ''Sm structure'' has been poorly studied up to now. Hcp samarium has been shown to exhibit a ferromagnetic transition below 165 K:[7] the magnetic moments, all localized on hexagonal sites, order along the *c* direction. The higher transition temperature is likely due to stronger coupling between the hexagonal planes that are no longer separated by cubic ones. In metastable dhcp samarium prepared under 40 kbar, a shift of the Néel ordering temperature of the cubic sites has been detected by magnetization measurements.[8] However, the magnetic structure of dhcp samarium is yet to be determined, probably because of the difficulty of preparing this phase, particularly as a single crystal.

Recently, high-quality dhcp (001) Sm single-crystals films have been prepared using molecular-beam epitaxy.[9] The form of these samples makes it possible to perform neutron-scattering measurements, even with natural Sm, because the single-crystal nature of the sample maximizes the reflected intensity while its small thickness (a few hundred nanometers) minimizes absorption. The samples are also well suited for resonant x-ray magnetic scattering (RXMS) experiments, since the enhancement by one to two orders of magnitude of the x-ray magnetic scattered intensity near the rare-earth absorption edges[10] allows polarization analysis at the Sm L_3 edge. In this paper we describe the first determination of the magnetic structure of dhcp Sm by using both these techniques applied to a 7500 Å dhcp (001) Sm film.

EXPERIMENT

The sample was prepared by molecular-beam epitaxy in a vacuum chamber whose base pressure was about 4

$\times 10^{-11}$ Torr. It was grown on a (110) sapphire substrate, previously subjected to a cleaning treatment and then heated to 850 °C for one hour in the growth chamber. Following the method proposed by Kwo *et al.*,[11] the substrate was first covered by a 500 Å niobium buffer layer deposited at 800 °C. To initiate the dhcp growth of samarium, a thin (001) Nd template layer (20 Å thick) was grown on the niobium buffer.[9] Samarium was then evaporated from an effusion cell on the substrate kept at 300 °C. The evaporation rate was controlled using a quartz monitor. The total film thickness was 7500 Å. Finally, a 500-Å-thick niobium layer was deposited on the top of the sample, in order to avoid further oxidation of the light rare earth.

In-situ reflection high-energy electron-diffraction patterns exhibit thin and continuous streaks, which confirms the 2D coherence and the single-crystal quality of the deposited layers. The epitaxial relationships are: $(1\bar{1}0)Al_2O_3$ // (110)Nb // (001)Nd //(001)Sm with [001]Nb // $[\bar{1}20]$Nd // $[\bar{1}20]$Sm and $[\bar{1}\bar{1}0]$Nb // [100]Nd // [100]Sm.

X-ray scattering curves obtained with the wave-vector transfer along the $[00l]$ and $[10l]$ directions show that the film grows in the dhcp structure with $c=11.673$ Å. It proved to be very homogeneous with a mosaic spread of 0.28 deg and a coherence length in stacking of the close-packed planes around 700 Å.

Neutron-scattering experiments were performed on the IN20 triple-axis spectrometer at Institut Laue Langevin. The neutron wavelength was 2.36 Å. The collimation was 30′ before and 40′ after the sample. The sample was mounted in a variable temperature He flow cryostat allowing measurements in the 1.5–300 K temperature range.

The RXMS experiments were performed at the bending magnet beamline BM28 (UK CRG) at the European Synchrotron Radiation Facility. The incident photon flux was 1.7 10^{11} photons/s at 200 mA with an incident degree of linear polarization perpendicular to the scattering plane (σ polarization) of 95%. The sample was mounted in a closed-cycle refrigerator on a diffractometer that allows experiments with four-circle geometry and polarization analysis of the scattered beam. Polarization analysis was performed using the (220) reflection of a Cu crystal. At the L_3 edge of samarium, the Bragg angle of the Cu(220) was 46.6 deg, resulting in a leakage of the order of 3 10^{-3}. The peak reflectivity of the analyzer was 3.5%. All the measurements were performed in the σ-π channel, i.e., selecting the polarization of the scattered beam that was rotated by 90 deg, in order to reduce the charge scattering background.[10]

MAGNETIC ORDERING OF THE HEXAGONAL SITES

At room temperature, neutron-scattering experiments performed with the wave-vector transfer along $(00l)$ and $(10l)$ confirmed that the film grows in the dhcp structure. The observed nuclear peaks are represented by black dots in the dhcp reciprocal lattice, Fig. 1. No significant change in the intensity of the peaks was measured, nor were any additional reflections observed on cooling the sample down to 25 ± 1 K. Below 25 K, a clear increase in the intensity of all

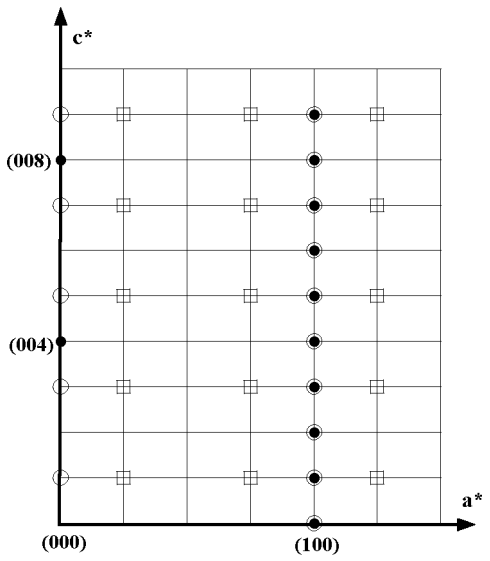

FIG. 1. Reciprocal lattice of dhcp Sm showing the positions for: nuclear (charge) scattering (filled circle), magnetic scattering from the hexagonal sites (empty circles), magnetic scattering from the cubic sites (empty squares).

the peaks in the $(10l)$ scan was observed, as illustrated in Fig. 2(a) presenting the (100) reflection at 130 K and 4.5 K. The thermal evolution of the integrated intensity measured for the same reflection is presented in Fig. 2(b). The increase of the background observed at low temperature has been

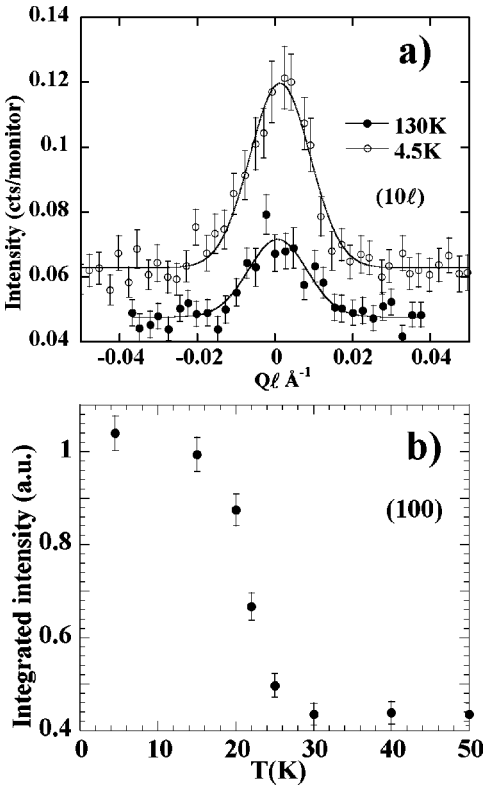

FIG. 2. (a) Neutron-scattering patterns collected at 130 K and 4.5 K around the (100) reflection for a 7500 Å dhcp (001)Sm film; (b) corresponding thermal evolution of the integrated intensity.

TABLE I. Ratios $R_{hex.}=I_{(hkl)}/I_{(100)}$: experimental values measured at 4.5 K and 130 K from neutron scattering and corresponding calculated values.

Reflection	4.5 K Expt.	Calc. (nuclear + magnetic)	130 K Expt.	Calc. (nuclear)
(100)	1 ± 0.2	1	1 ± 0.2	1
(101)	1.4 ± 0.2	1.37	2.65 ± 0.4	2.95
(102)	4.0 ± 0.6	4.02	8.2 ± 0.9	8.83
(103)	1.1 ± 0.2	1.31	2.2 ± 0.2	2.94
(104)	0.7 ± 0.2	0.71	0.7 ± 0.2	1

shown to be related to sample environment. Let us underline that the lack of supplemental contributions below 25 K along $(00l)$, reveals that the magnetic moments are aligned along the c axis. The experimental ratios $R_{hex.}=I_{(hkl)}/I_{(100)}$ (I are integrated intensities) measured at 130 K and 4.5 K are listed in Table I. The corresponding calculated ratios, considering only nuclear scattering at high temperature, and including both nuclear and magnetic scattering at low temperature are also given.

The magnetic scattering has been calculated assuming, by analogy with the magnetic structure of bulk Sm, that (1) magnetic moments align along the c axis [consistent with rule (i)]; (2) the coupling within each hexagonal plane is ferromagnetic [consistent with rule (ii)]; and (3) the coupling between hexagonal planes separated by a cubic plane is antiferromagnetic leading to a $+0-0+$ sequence along the c direction (Fig. 3).

The data were fitted with the same form factor as in Ref. 4 and calculated from the dipole approximation. Rather good agreement between the calculated and experimental intensity ratios is obtained. As was pointed out in this reference, the magnetic moment of Sm arises from a delicate balance between oppositely directed spin and orbital moments. It was found that the present data could be fitted with the same combination of spin and orbital moments as was found in Sm thin films with the Sm structure,[4] this corresponds to $L=5$, $S=-1.9$ giving a $4f$ moment of $1.2\mu_B/\text{atom}\pm0.2\mu_B$. The data are not very sensitive to moments due to polarization of $5d$ electrons, since they only cover a range of q in which the $5d$ form factor is relatively small. The $4f$ moments value is thus significantly higher than the magnetic moment of samarium, which includes all the magnetic contributions. In summary, for dhcp samarium, the magnetic ordering in individual hexagonal planes is the same as in bulk samarium, whereas the 3D magnetic ordering is modified by the change in the sequence of the stacked planes (Fig. 3). The resulting propagation vector is $\tau_h=(001)$ (empty circles in Fig. 1).

The magnetic reflections measured by neutron scattering could not be observed by RXMS, since they are at the same positions in the reciprocal space as very intense charge reflection from the dhcp structure. With RXMS, we thus concentrate on the specular (007) magnetic reflection (not observable with neutrons because of the alignment of the magnetic moment parallel to the scattering vector) and we

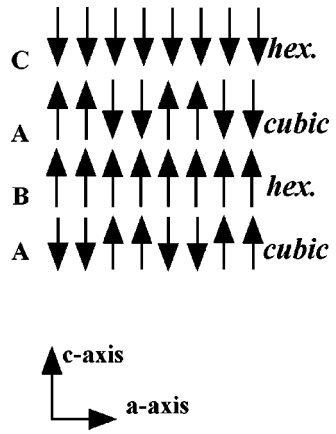

FIG. 3. Sketch of the magnetic arrangement in dhcp samarium.

measured a clear and sharp drop in the magnetic intensity around 25 K, confirming the above neutron-scattering results. Some remaining contribution was actually observed above this temperature; although it is likely due to experimental artifacts (multiple scattering), further experiments are still necessary for confirmation.

MAGNETIC ORDERING OF THE CUBIC SITES

Neutron-scattering experiments were performed at 1.5 K in order to investigate the magnetic ordering of the cubic sites. At this temperature a new magnetic peak around the (1.25 0 1) reflection (empty square in Fig. 1) with a very low intensity (around 10 counts/min) could be observed. This reflection is attributed to magnetic ordering of the cubic sites as described below. However, because of the very low counting rate and the consequent prohibitive measurement time, it was not possible to undertake a detailed study of the cubic site ordering by neutron diffraction.

The magnetic ordering of the cubic sites has been investigated in detail using RXMS. It was established that the magnetic ordering on these sites occurs at 24 ± 1 K, with the

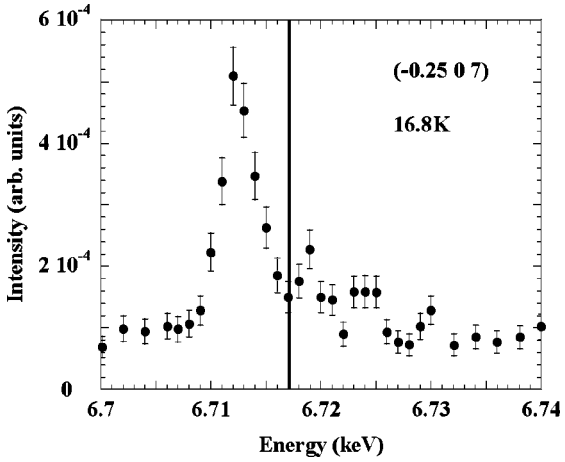

FIG. 4. Energy dependence of the peak intensity measured at the $(-0.25\ 0\ 7)$ reflection, at 16.8 K for a 7500 Å dhcp (001)Sm film. The vertical line corresponds to the Sm L_3 absorption edge.

TABLE II. Ratios $R_{cub.}=I_{(hkl)}/I_{(-0.25\ 0\ 7)}$: experimental values measured at 8.8 K from RXMS experiments and corresponding calculated values.

Reflection	8.8 K Expt.	Calc.
$(-0.25\ 0\ 7)$	1 ± 0.08	1
$(-0.75\ 0\ 7)$	0.76 ± 0.2	0.75
$(-1.25\ 0\ 7)$	0.36 ± 0.06	0.25
$(-1.75\ 0\ 7)$	0 ± 0.2	0.02

appearance of magnetic intensity in the $(0.25+0.5n,\ 0,\ 2m+1)$ reflections (n and m are integers). As in Sm with the Sm structure,[12] the energy dependence shows a strong maximum below the edge, attributed to quadrupolar ($4f$) resonance, and some structures above the edge, corresponding to dipolar ($5d$) resonance (Fig. 4). We measured several magnetic reflections at the $4f$ resonance (4 eV below the samarium L_3 edge). As an example, Fig. 5 shows the $(-0.25\ 0\ 7)$ magnetic peak at various temperatures and the thermal evolution of its integrated intensity. The peak position slightly changes when the temperature increases because of thermal contraction of the sample [the same variation is observed for the (008) charge peak]. The experimental ratios between the integrated intensities, $R_{cub.}=I_{(hkl)}/I_{(-0.25\ 0\ 7)}$, measured at 8.8 K for three peaks located close to the (007) reflection, are listed in Table II.

Similarly to the hexagonal sites, the magnetic structure of the cubic sublattice can be guessed by analogy with bulk samarium. However, for these sites, two different structures [that follow the rules (i) and (iv) given for the Sm structure in the Introduction] should be considered. Depending on the basal planes coupling, either a $\boldsymbol{\tau}_{c1}=(0.25\,0\,1)$ or a $\boldsymbol{\tau}_{c2}=(0.25\ 0\ 0.5)$ propagation vector could be expected. As reported above, we observed several reflections corresponding to $\boldsymbol{\tau}_{c1}$ (empty squares in Fig. 1), and none corresponding to $\boldsymbol{\tau}_{c2}$; thus, the experimental results lead to the magnetic structure sketched in Fig. 3. The intensities calculated using the Hannon *et al.* theory based on the atomic approximation[10] (for details see Ref. 12) are presented in Table II for the same reflections as the experimental ones. The calculated intensities are in qualitative agreement with the experimental data.

In dhcp samarium, the magnetic ordering *in* individual cubic planes is therefore the same as in bulk samarium, while the magnetic ordering *between* the planes, characterized by a propagation vector $\boldsymbol{\tau}_{c1}=(0.25\ 0\ 1)$ (Fig. 1), is modified (Fig. 3).

DISCUSSION

Samarium crystallizing with the dhcp crystal structure undergoes a magnetic transition at about 25 K in which the hexagonal and cubic sites order nearly simultaneously. The ordering temperature of the hexagonal sites is thus lowered compared to bulk Sm; this could be related to the dhcp stacking, where each hexagonal plane is isolated (they are separated by cubic ones), which likely reduces the interaction between pairs of h planes. Conversely, the ordering temperature of the cubic sites increases; this could be also attributed to the dhcp stacking, since cubic planes are in this case closer to each other than in the samarium structure (they are separated by only one instead of two hexagonal planes), giving probably rise to a stronger interaction. The coupling between the two kinds of sites, even if it is weak, could also lead to the convergence of the two magnetic transitions.

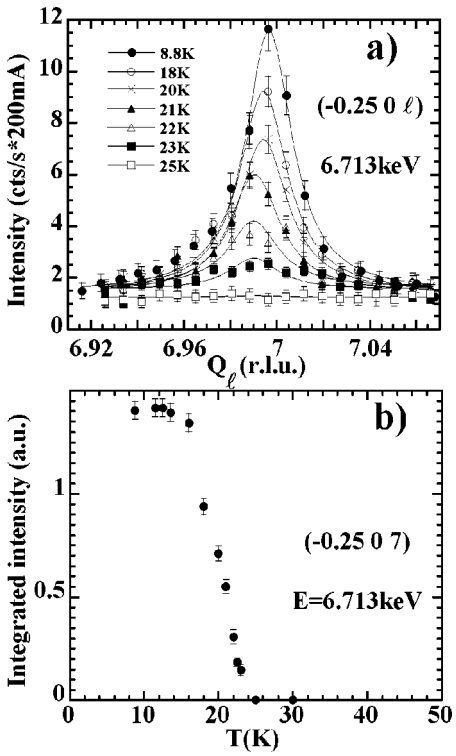

FIG. 5. (a) RXMS patterns collected at various temperatures between 8.8 K and 25 K around the $(-0.25\ 0\ 7)$ reflection for a 7500 Å dhcp (001)Sm film; (b) corresponding thermal evolution of the integrated intensity.

This study of the magnetic structure in dhcp samarium should be now complemented by the analysis of the magnetic resonance process. The aim would be to observe the $5d$ band polarization, in comparison with the results obtained for samarium with the Sm structure (Refs. 5 and 12), in order to study correlations between the $5d$ band polarization and the distance between hexagonal or cubic magnetic planes. Finally, the elaboration of films of dhcp samarium is the first step towards growing dhcp Sm/Nd or Sm/La superlattices. Such artificially modulated structures should permit studies of the magnetic coherence between both hexagonal and cubic sites through different spacers with similar dhcp stacking.

[1] A. H. Daane, R. E. Rundle, H. G. Smith, and F. H. Spedding, Acta Crystallogr. **7**, 534 (1954).
[2] W. C. Kohler and R. M. Moon, Phys. Rev. Lett. **29**, 1468 (1972).
[3] S. L. Lee *et al.*, J. Magn. Magn. Mater. **127**, 145 (1993).
[4] K. Dumesnil, C. Dufour, Ph. Mangin, M. Hennion, and P. J. Brown, Phys. Rev. B **60**, 10 743 (1999).
[5] K. Dumesnil, C. Dufour, Ph. Mangin, and A. Stunault, J. Phys.: Condens. Matter **12**, 3091 (1999).
[6] B. R. Coles, J. Less-Common Met. **77**, 153 (1981).
[7] H. Adachi, K. Kimura, and H. Ino, Mater. Sci. Eng., A **181**, 864 (1994).
[8] A. Jayaraman and R. C. Sherwood, Phys. Rev. **134**, A692 (1964).
[9] C. Dufour, K. Dumesnil, S. Soriano, D. Pierre, Ch. Senet, and Ph. Mangin, J. Cryst. Growth **234**, 447 (2002).
[10] J. P. Hannon, G. T. Trammell, M. Blume, and D. Gibbs, Phys. Rev. Lett. **61**, 1245 (1988).
[11] J. Kwo, M. Hong, and S. Nakahara, Appl. Phys. Lett. **49**, 319 (1986).
[12] A. Stunault, K. Dumesnil, C. Dufour, C. Vettier, and N. Bernhoeft, Phys. Rev. B **65**, 064436 (2002).